Thallium-205 and Carbon-13 NMR Studies of Human Sero- and Chicken Ovotransferrin†

James M. Aramini,‡ Peter H. Krygsman,§ and Hans J. Vogel*,‡

Division of Biochemistry, Department of Biological Sciences, University of Calgary, Calgary, Alberta, Canada T2N 1N4, and Bruker Spectrospin (Canada) Ltd., 555 Steeles Avenue East, Milton, Ontario, Canada L9T 1Y6

Received November 24, 1993⊛

ABSTRACT: We have examined the binding of Tl^{3+} to human serotransferrin and chicken ovotransferrin in the presence of carbonate and oxalate by ^{205}Tl and ^{13}C NMR spectroscopy. With carbonate as the synergistic anion, one observes two ^{205}Tl NMR signals due to the bound metal ion in the two high-affinity iron-binding sites of each protein. When the same adducts are prepared with ^{13}C-labeled carbonate, one finds two closely spaced doublets in the carbonyl region of the ^{13}C NMR spectrum of serotransferrin; these correspond to the labeled anion directly bound to the metal ion in both sites of the protein. The analogous resonances in ovotransferrin are completely degenerate, and only one doublet can be detected. The magnitudes of the spin–spin coupling between the bound metal ion and carbonate range from $^2J(^{205}Tl–^{13}C) \approx 270$ to 290 Hz. We have used the proteolytic half-molecules of ovotransferrin and the recombinant N-terminal half-molecule of serotransferrin to assign the ^{205}Tl and ^{13}C NMR signals due to the bound metal ion and anion in both proteins. From titration studies, we found that Tl^{3+} is bound with a greater affinity at the C-terminal site of serotransferrin, whereas no site preference can be noted for ovotransferrin. When oxalate is used as the anion instead of carbonate, the ^{205}Tl NMR signals arising from the bound metal ion in the sites of ovotransferrin are shifted downfield and become almost degenerate. A very complex pattern of resonances is observed for bound $^{13}C_2O_4^{2-}$ in the ^{13}C NMR spectra of both proteins. From studies of the $Tl^{3+}/^{13}C_2O_4^{2-}$ adducts of the half-molecules of ovotransferrin and the N-terminal lobe of serotransferrin at two magnetic fields, we have shown that the ^{13}C NMR signals for the carbonyl carbons due to bound oxalate in each site are split into a doublet of doublets by carbon–carbon [$^1J(^{13}C–^{13}C) \approx 70–75$ Hz] and thallium–carbon [$^2J(^{205}Tl–^{13}C) \approx 15–30$ Hz) spin–spin couplings. These results suggest that oxalate binds to Tl^{3+} in a 1,2-bidentate manner in both transferrins. Finally, from field dependence studies we found that the line widths of the ^{205}Tl NMR signals for the Tl^{3+}/carbonate forms of ovo- and serotransferrin increase dramatically with increasing external magnetic field strength (B_0). We have determined that these effects can be attributed to nuclear relaxation via the chemical shift anisotropy (CSA) mechanism and calculated a value of the chemical shift anisotropy for serotransferrin-bound Tl^{3+} of $\Delta\sigma = 680$ ppm. These findings have important ramifications concerning the potential of ^{205}Tl and other heavy $I = {}^1/_2$ metal nuclei to study metalloproteins by NMR spectroscopy.

Transferrins are a family of large (MW ≈ 80 000) iron-binding glycoproteins that are of vital importance to the transport and regulation of iron in mammals [for recent reviews, see Baker and Lindley (1992), de Jong *et al.* (1990), Harris and Aisen, (1989), Heubers and Finch (1987), and Brock (1985)]. The three major types of transferrins—serotransferrin (sTf),[1] a prominent serum protein, ovotransferrin (OTf), found in avian egg white, and lactoferrin (lTf), present in milk and other secretory fluids—are highly homologous (Metz-Boutigue *et al.*, 1984) bilobal monomers, with each lobe containing one Fe^{3+}-binding site. These sites chelate Fe^{3+} with remarkably high affinity ($K_D \leq 10^{-20}$ M^{-1}), yet at the same time reversibly. In order to attain such traits, nature has designed an elegant system that is unique to transferrins, in which a synergistic anion (carbonate) is both required and directly involved in the metal binding process. A number of other anions (for example, oxalate) may also fulfill the role of carbonate *in vitro*. The high-affinity Fe^{3+}-binding sites of transferrins also exhibit a rather broad metal ion specificity, illustrated by the number of diverse metal ions that can bind to these proteins. Several years ago, it was postulated that the synergistic anion must possess a carboxylate moiety flanked by a second electron donor group, and that it binds directly to the metal ion and interacts simultaneously with basic protein residue(s) in the site (the interlocking sites model; Schlabach & Bates, 1975).

In recent years, a much more lucid picture of the nature and properties of the metal ion binding sites in transferrins has been obtained by spectroscopic investigations, and to this end two of the most powerful techniques have proven to be X-ray crystallography and NMR spectroscopy. Over the last decade, several studies established three general approaches for the use of NMR to monitor metal ion binding to these

† This research was supported by the Medical Research Council of Canada (MRC). The AM 400 and AMX 500 NMR spectrometers used in this work were purchased with funds provided by the MRC and the Alberta Heritage Foundation for Medical Research (AHFMR). J.M.A. is the recipient of a studentship from the AHFMR. H.J.V. is an AHFMR scholar.

* To whom correspondence should be addressed.
‡ University of Calgary.
§ Bruker Spectrospin (Canada) Ltd.

⊛ Abstract published in *Advance ACS Abstracts,* March 1, 1994.

[1] Abbreviations: sTf, serotransferrin; OTf, ovotransferrin; lTf, lactoferrin; NMR, nuclear magnetic resonance; OTf/2N, N(amino)-terminal half-molecule of ovotransferrin; OTf/2C, C(carboxy)-terminal half-molecule of ovotransferrin; TPCK, L-1-tosylamido-2-phenylethyl chloromethyl ketone; sTf/2N, N(amino)-terminal half-molecule of serotransferrin; EDTA, ethylenediaminetetraacetic acid; TMS, tetramethylsilane; MES, 2-(*N*-morpholino)ethanesulfonic acid; ESEEM, electron spin echo envelope modulation.

0006-2960/94/0433-3304$04.50/0

proteins: (1) direct detection of bound diamagnetic metal ions, such as Al^{3+} (Aramini & Vogel, 1993a,b; Aramini *et al.*, 1993), Sc^{3+} (Aramini & Vogel, 1994), VO_2^+ (Butler *et al.*, 1987; Butler & Eckert, 1989), Cd^{2+} (Sola, 1990a,b; Battistuzzi & Sola, 1992), and Tl^{3+} (Bertini *et al.*, 1983), (2) observation of bound ^{13}C-enriched anions such as $^{13}CO_3^{2-}$ and $^{13}C_2O_4^{2-}$ (Zweier *et al.*, 1981; Bertini *et al.*, 1986, 1988), and (3) the use of ^1H NMR to follow the conformational changes induced by metal ion binding (Kubal & Sadler, 1992; Kubal *et al.*, 1992, 1993). Taken together, these studies have confirmed the existence of a direct bond between the synergistic anion and the bound metal ion and have uncovered differences in the environment and behavior of the metal ion binding sites within the same protein and/or different transferrins. The X-ray structures of the Fe^{3+}/carbonate forms of human lTf (Anderson *et al.*, 1987, 1989) as well as rabbit sTf and its N-terminal half-molecule (Bailey *et al.*, 1988; Sarra *et al.*, 1990) established that the high-affinity iron-binding sites are situated in deep interdomain clefts in both lobes of the protein, and that the side chains of four highly conserved residues—1 Asp, 1 His, and 2 Tyr—along with two oxygens from the synergistic anion serve as ligands for the bound metal ion. Furthermore, X-ray crystal data for oxalate bound to Cu^{2+} in the C-terminal site of intact human lTf showed that this larger anion binds in a 1,2-bidentate fashion, leading to a modification of the interlocking sites model (Smith *et al.*, 1991; Shongwe *et al.*, 1992). X-ray techniques have also demonstrated that significant conformational changes occur during the transition between the apo- (open) and holo- (closed) forms of several transferrins (Anderson *et al.*, 1990; Grossmann *et al.*, 1992, 1993).

In this report, we have used ^{13}C and ^{205}Tl NMR spectroscopy to study the binding of Tl^{3+} to human sTf and chicken OTf and their half-molecules. In aqueous media, thallium can exist in one of two oxidation states, Tl^+ and Tl^{3+} (the latter is readily reduced to the +1 state), and it is the ability of Tl^+ to mimic alkali metal ions, especially K^+, that is the root of this metal's toxicity and, thus, its biological relevance [recently reviewed by Douglas *et al.* (1990)]. Thallium has two stable nuclear spin $I = {}^1/_2$ isotopes, ^{203}Tl and ^{205}Tl, and is one of the only metals in the entire periodic table that features both a diamagnetic +3 cation and at least one $I = {}^1/_2$ isotope that is amenable to study by NMR. Both ^{203}Tl and ^{205}Tl possess several excellent NMR properties, such as high resonance frequency and high sensitivity, though the latter is slightly superior due to its natural abundance (70.5%) and thus is the commonly studied isotope of this element [for recent reviews, see Hinton (1992) and Hinton *et al.* (1988)]. The ^{205}Tl chemical shift is extremely sensitive to the chemical environment of the metal ion, as reflected by the vast chemical shift range of this nucleus (≈7000 ppm). In addition, spin–spin coupling between ^{205}Tl and $I = {}^1/_2$ nuclei in complexes of Tl^+ and Tl^{3+} may be quite large and can give information about the coordination of ligands to the metal ion. Despite the relatively large ionic radius of Tl^{3+} ($r \approx 0.89$ Å; Shannon, 1976), ^{205}Tl NMR spectroscopy is a potentially excellent probe for the metal ion binding sites of metalloproteins, in particular Fe^{3+}-binding proteins. However, because of its biological importance, Tl^+ has been the focus of virtually all the biochemical applications of ^{205}Tl NMR, and the low-field study of Tl^{3+} binding to human sTf (Bertini *et al.*, 1983) stands as the only published example to date of the use of this technique to investigate Tl^{3+} binding to a protein.

EXPERIMENTAL PROCEDURES

Materials. Human apo-sTf and chicken apo-OTf were purchased from Sigma Chemical Co. and used without further purification. The N- and C-terminal half-molecules of OTf (OTf/2N and OTf/2C) were isolated from the mild digestion of diferric OTf (Sigma Chemical Co.) with TPCK-treated trypsin and characterized following published procedures (Oe *et al.*, 1988; Nakazato *et al.*, 1992; Thornton *et al.*, 1989). The recombinant N-terminal half-molecule of human sTf (sTf/2N), expressed in baby hamster kidney cells and purified as previously described (Funk *et al.*, 1990; Mason *et al.*, 1991), was kindly donated to us by Dr. A. B. Mason and Dr. R. C. Woodworth, University of Vermont College of Medicine. This half-molecule was deferrated by dialysis against 0.1 M citrate, pH 4.7, followed by 0.1 M $NaClO_4$, prior to exchanging the sample into the buffer of choice using a Spectrum ultrafiltration system. The dihydrate of thallic chloride ($TlCl_3 \cdot 2H_2O$) was obtained from Aldrich Chemical Co. ^{13}C-enriched (99%) sodium carbonate ($Na_2{}^{13}CO_3$) and sodium oxalate ($Na_2{}^{13}C_2O_4$) were purchased from MSD Isotopes. D_2O (99.9%) was obtained from Cambridge Isotopes Laboratories. All other chemicals used in this study were of the highest quality available.

Stock solutions of Tl^{3+} (ca. 100 mM, pH 3) were standardized by complexometric back titration in the following way: a known amount of EDTA was added to an aliquot of the Tl^{3+} stock and, under alkaline conditions, the amount of excess chelator was determined by addition of Mg^{2+} with Eriochrome black T as the indicator (Bertini *et al.*, 1983; Skoog & West, 1982). The concentrations of the protein NMR samples (each ≈ 2 mL and containing 25% v/v D_2O for a lock) were determined spectrophotometrically using the following extinction coefficients: ϵ_{280} (M^{-1} cm^{-1}): apo-OTf, 91 200; apo-sTf, 92 300; apo-OTf/2N, 43 800; apo-OTf/2C, 40 300; apo-sTf/2N, 38 600 (Luk, 1971; Oe *et al.*, 1988; Funk *et al.*, 1990). Samples were adjusted to the desired pH as outlined in our earlier studies with OTf (Aramini & Vogel, 1993a).

NMR Spectroscopy. ^{205}Tl NMR spectra were acquired unlocked and at 25 °C on two instruments, a Bruker MSL 100 (ν_0 = 57.7 MHz) and a Bruker AC 200 (ν_0 = 115.5 MHz), each equipped with a 10-mm broad-band probe. In both cases, it was necessary to employ a probe head from a higher field instrument (≥300 MHz) in order to tune to the appropriate frequency. Typical acquisition parameters are as follows: a 60–70° flip angle, a repetition time of 1 s, a sweep width of 50 kHz, and 8K complex points (16K total). All data were processed with a 100-Hz line broadening. The line widths of ^{205}Tl NMR signals were obtained by fitting each spectrum using the LINESIM routine (P. Barron, Bruker Australia) on an ASPECT 1000 computer. ^{205}Tl NMR spectra are referenced to the signal due to bound Tl^{3+} in the C-site of sTf (δ = 2055 ppm with respect to Tl^+ at infinite dilution; Bertini *et al.*, 1983). Proton-coupled ^{13}C NMR spectra of the proteins used in this study were acquired locked and at 25 °C on Bruker AM 400 (100.6 MHz) and AMX 500 (125.7 MHz) spectrometers using parameters listed elsewhere (Aramini & Vogel, 1993a) and processed with a 3–7-Hz line broadening. ^{13}C NMR spectra are referenced to internal dioxane (δ = 67.40 ppm with respect to TMS).

RESULTS

Tl^{3+} Binding to sTf in the Presence of Carbonate. When Tl^{3+} is added to a solution of human apo-sTf containing an

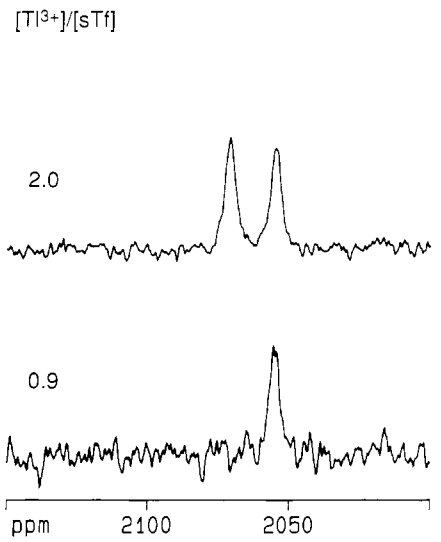

FIGURE 1: ^{205}Tl (115.5 MHz) NMR spectra of human sTf plus varying amounts of Tl^{3+}. (Lower trace) 1.01 mM sTf, 0.10 M KCl, 20 mM $Na_2{}^{13}CO_3$, 0.9 equiv of Tl^{3+}, pH 7.3, 87 000 scans; (upper trace) 1.09 mM sTf, 0.15 M KCl, 0.15 M $NaHCO_3$, 2.0 equiv of Tl^{3+}, pH 7.9, 58,400 scans.

excess of carbonate, two signals at δ = 2055 and 2072 ppm appear sequentially in the ^{205}Tl NMR spectrum (Figure 1). These resonances correspond to Tl^{3+} bound in a ternary complex to carbonate and the protein in the high-affinity Fe^{3+}-binding sites of sTf. The binding of Tl^{3+} to sTf and OTf (*vide infra*) is accompanied by a change in the color of the sample to yellow, irrespective of the synergistic anion. When the identical experiment is performed with ^{13}C-labeled anion and monitored by ^{13}C NMR, one doublet emerges at δ = 166.22 ppm [$^2J(^{205}Tl-^{13}C)$ = 285 Hz] upon addition of the first equivalent of Tl^{3+}, followed by a second doublet slightly upfield of the first [δ = 165.98 ppm; $^2J(^{205}Tl-^{13}C)$ = 268 Hz] when the protein is saturated with the metal ion (Figure 2). The signal at $\delta \approx$ 164.5 ppm due to bound carbonate in the site(s) of sTf in the absence of metal ion (Zweier *et al.*, 1981) disappears during the titration. The peak separations in frequency units (Hz) for the signals comprising both ^{13}C doublets do not change when the experiment is performed on a higher field instrument, confirming that the pattern obtained is a result of spin–spin coupling between the metal ion and labeled carbonate (Bertini *et al.*, 1988).[2]

The ^{205}Tl and ^{13}C signals for the $Tl^{3+}/{}^{13}CO_3^{2-}$ form of sTf have been assigned on the basis of their pH dependence and with the recombinant N-terminal half-molecule of this protein. When the pH of a solution of $(Tl^{3+})_2$–sTf-$(^{13}CO_3^{2-})_2$ is dropped from pH 7.6 to 6.3, only one of the doublets remains in the ^{13}C NMR spectrum (Figure 3a,b). This signal corresponds to metal-bound carbonate in the acid stable C-site of the protein (i.e., Evans & Williams, 1978; Harris, 1977). The other (low frequency) doublet is observed for the analogous adduct of sTf/2N (Figure 3c). Taken together with the ^{205}Tl and ^{13}C titration data, we can assign the ^{205}Tl signals and conclude that Tl^{3+} binds preferentially to the C-terminal site of sTf when carbonate serves as the synergistic anion. Our ^{205}Tl and ^{13}C NMR results for sTf (shown in Table 1) are in good agreement with those of Bertini *et al.* (1983, 1988), except that these authors incorrectly assigned the ^{13}C signals on the basis of results obtained for a monoferric monothallium derivative of the protein.

[2] Since the magnetogyric ratios (γ) of ^{205}Tl and ^{203}Tl are very similar, the magnitudes of the spin–spin coupling involving each isotope [i.e., $^2J(^{205}Tl-^{13}C)$ and $^2J(^{203}Tl-^{13}C)$] are virtually identical, and thus it is difficult to distinguish the coupling due to the less abundant ^{203}Tl.

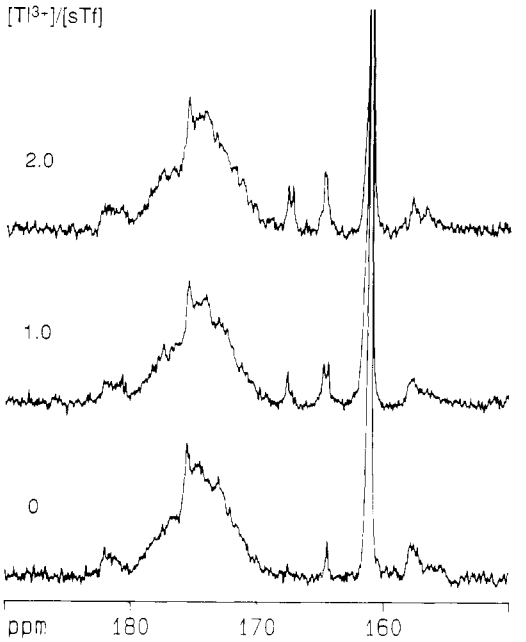

FIGURE 2: ^{13}C (100.6 MHz) NMR spectra of human sTf (1.07 mM, 20 mM $Na_2{}^{13}CO_3$, pH 7.6) in the presence of 0, 1.0, and 2.0 equiv of Tl^{3+}; 20 000 scans each. Only the carbonyl region of each spectrum is shown. The signal at δ = 161.1 ppm corresponds to excess ^{13}C-labeled bicarbonate. The envelope of resonances at $\delta \approx$ 170–183 ppm as well as the peak at δ = 157.8 ppm are due to natural abundance ^{13}C in the backbone and side-chain carbonyls and the guanidinium group of Arg residues in the protein, respectively.

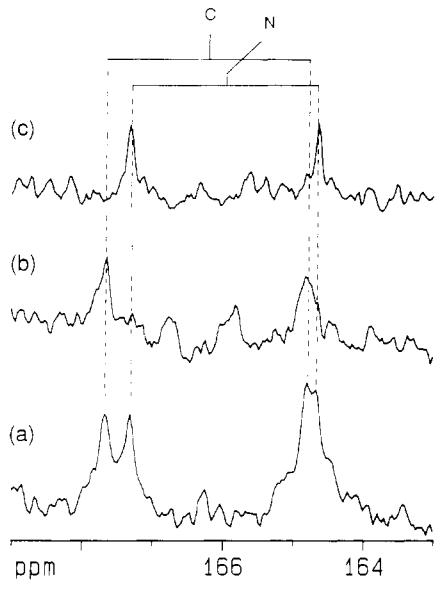

FIGURE 3: Expanded carbonyl regions of the ^{13}C (100.6 MHz) NMR spectra of (a) 1.07 mM human sTf in the presence of 20 mM $Na_2{}^{13}CO_3$ and 2.0 equiv of Tl^{3+} at pH 7.6; 20 000 scans; (b) sample from trace a at pH 6.3 (20 mM MES); 20 000 scans; (c) 0.13 mM sTf/2N in the presence of 1.0 equiv of Tl^{3+}, 5 mM $Na_2{}^{13}CO_3$, 0.1 M NaCl at pH 7.6; 64 700 scans.

Tl^{3+} Binding to OTf in the Presence of Carbonate. ^{13}C NMR spectra of the titration of chicken apo-OTf in the presence of an excess of ^{13}C-enriched carbonate with Tl^{3+} are shown in Figure 4. In contrast to the situation described above for sTf, only one doublet [δ = 165.92 ppm; $^2J(^{205}Tl-^{13}C)$ = 281 Hz], which increases in intensity up to 2 equiv of metal ion, is observed in the carbonyl region of the spectrum. Again, the frequency difference between the peaks in the degenerate

Table 1: ^{205}Tl and ^{13}C NMR Data for the Tl^{3+}/Carbonate Adducts of sTf, OTf, and Their Half-Molecules

protein	$\delta^{205}Tl$ (ppm)	δ ^{13}C (ppm)	$^2J_{(^{205}Tl-^{13}C)}$ (Hz)	assignment
sTf	2072	165.98	268	N-site
	2055	166.22	285	C-site
sTf/2N	nd	165.98	268	
OTf	2075	165.92	281	N-site
	2054	165.92	281	C-site
OTf/2N	2075	nd	nd	
OTf/2C	2054	nd	nd	

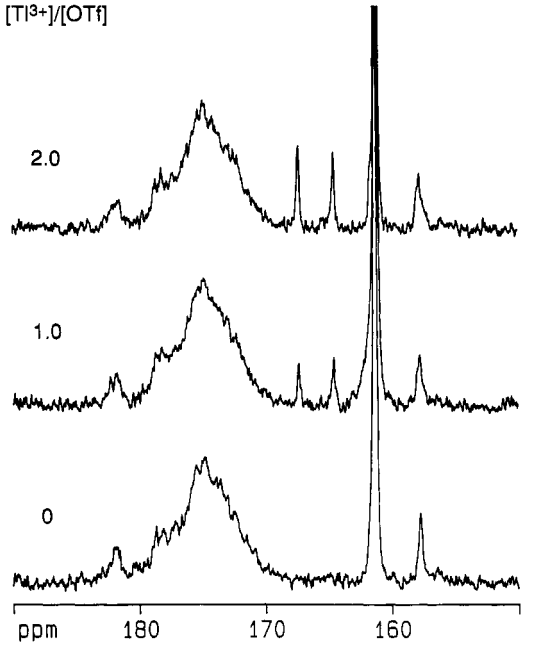

FIGURE 4: ^{13}C (100.6 MHz) NMR spectra of chicken OTf (1.11 mM, 20 mM $Na_2{}^{13}CO_3$, 0.1 M KCl, pH 7.8) in the presence of 0, 1.0, and 2.0 equiv of Tl^{3+}; 20 000 scans each. Only the carbonyl region of each spectrum is shown. Again, the signals at $\delta \approx 170$–183, 161.1, 157.8 ppm correspond to backbone and side-chain carbonyls in the protein, excess ^{13}C-labeled bicarbonate, and the guanidinium group of Arg residues in the protein, respectively.

doublets is not dependent on the external magnetic field, meaning that this separation is also due to spin–spin coupling between ^{205}Tl and the ^{13}C-labeled anion directly bound to it. In the ^{205}Tl NMR spectrum of $(Tl^{3+})_2$–OTf–$(CO_3^{2-})_2$ two distinct ^{205}Tl NMR signals (δ = 2075 and 2054 ppm) are detected, corresponding to bound Tl^{3+} in both sites of OTf (Figure 5). ^{205}Tl NMR experiments on the Tl^{3+}/carbonate forms of OTf/2N and OTf/2C afford a conclusive assignment of the signals for the native protein. Bound Tl^{3+} in OTf/2C gives a signal that lines up perfectly with the low frequency resonance in the intact protein, while the high frequency signal was obtained for Tl^{3+}–OTf/2N–CO_3^{2-} (Figure 5). From titration studies followed by ^{205}Tl NMR, we found no evidence for a difference in the affinities of the two metal ion binding sites of OTf for Tl^{3+} (data not shown). Also, the rather large $^2J(^{205}Tl-^{13}C)$ coupling constants found by ^{13}C NMR were not discernable in the ^{205}Tl NMR spectra (B_0 = 4.7 T) of either OTf or sTf when ^{13}C-enriched carbonate was used (data not shown). The ^{205}Tl and ^{13}C NMR data for OTf and its half-molecules are included in Table 1.

Tl^{3+} Binding to OTf in the Presence of Oxalate. A very different scenario is found when the synergistic anion is changed to oxalate. In the ^{205}Tl NMR spectrum of the Tl^{3+}/oxalate adduct of OTf one observes two overlapping ^{205}Tl signals substantially downfield of those obtained in the experiments with carbonate (δ = 2103 and 2100 ppm; Figure 6). The signals are assigned to Tl^{3+} bound to oxalate and protein residues in the N- and C-terminal sites of OTf, respectively, based on the ^{205}Tl NMR spectrum of OTf/2C (Figure 6; Table 2). A very complex pattern of signals is observed in the carbonyl region of the ^{13}C NMR spectrum of $(Tl^{3+})_2$–OTf–$(^{13}C_2O_4^{2-})_2$ (Figure 7); somewhat simpler spec-

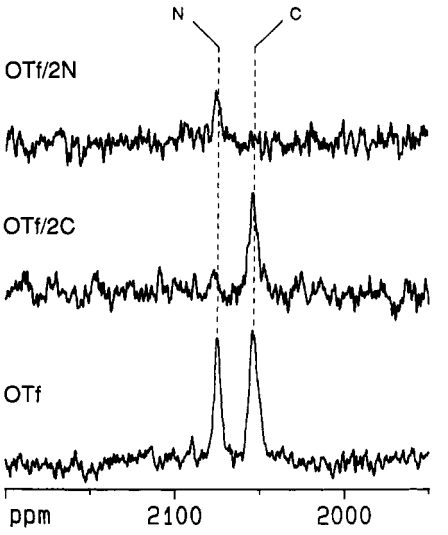

FIGURE 5: ^{205}Tl (115.5 MHz) NMR spectra of the Tl^{3+}/carbonate forms of OTf (1.20 mM, 2.0 equiv Tl^{3+}, 0.15 M KCl, 0.15 M $NaHCO_3$, pH 7.9, 41 500 scans), OTf/2C (0.44 mM, 0.9 equiv Tl^{3+}, 0.05 M Na_2CO_3, pH 7.6, 200 000 scans), and OTf/2N (0.15 mM, 0.9 equiv Tl^{3+}, 0.05 M Na_2CO_3, pH 7.8, 150 000 scans).

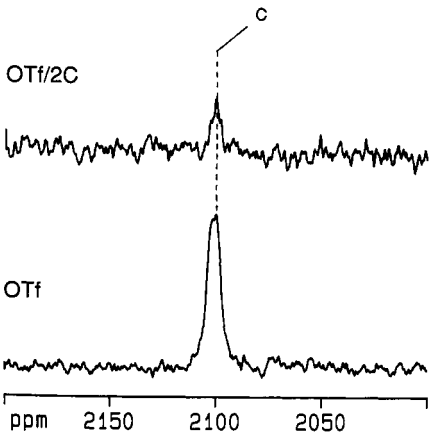

FIGURE 6: ^{205}Tl (115.5 MHz) NMR spectra of the Tl^{3+}/oxalate adducts of OTf (1.16 mM, 2.0 equiv Tl^{3+}, 0.10 M KCl, 10 mM $Na_2{}^{13}C_2O_4$, pH 7.7, 80 000 scans) and OTf/2C (0.25 mM, 0.9 equiv Tl^{3+}, 0.10 M KCl, 2.5 mM $Na_2{}^{13}C_2O_4$, pH 7.7, 168 000 scans).

Table 2: ^{205}Tl and ^{13}C NMR Data for the Tl^{3+}/Oxalate Adducts of OTf, OTf/2N, OTf/2C, and sTf/2N

protein	(a) ^{205}Tl NMR δ ^{205}Tl (ppm)	assignment[a]
OTf	2103	N-site
	2100	C-site

protein	(b) ^{13}C NMR δ ^{13}C (ppm)	$^1J_{(^{13}C-^{13}C)}$ (Hz)	$^2J_{(^{205}Tl-^{13}C)}$ (Hz)
OTf/2N	167.91	73	28
	165.99	73	14
OTf/2C	167.80	73	32
	165.35	73	21
sTf/2N	167.88	72	27
	165.62	72	15

[a] Based on ^{205}Tl NMR results for OTf/2C (Figure 6).

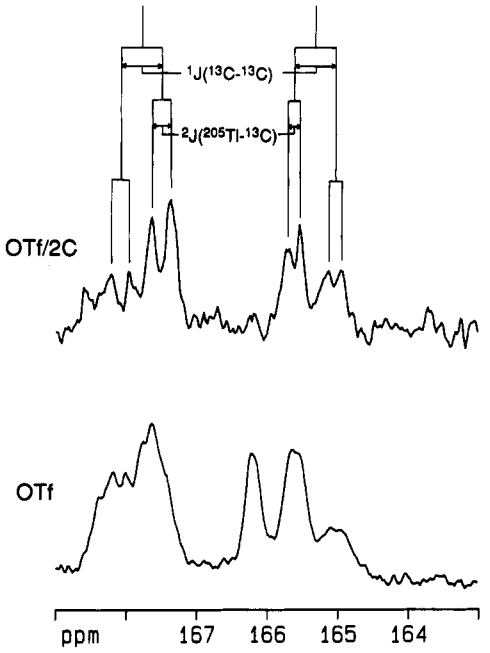

FIGURE 7: Expanded carbonyl regions of the ^{13}C (125.7 MHz) NMR spectra of the Tl^{3+}/oxalate forms of OTf (1.02 mM, 2.0 equiv Tl^{3+}, 0.10 M KCl, 10 mM $Na_2{}^{13}C_2O_4$, pH 7.7, 20 000 scans) and OTf/2C (0.31 mM, 0.9 equiv Tl^{3+}, 2.5 mM $Na_2{}^{13}C_2O_4$, pH 7.8, 40 000 scans).

tra are obtained for the Tl^{3+}/oxalate adducts of the half-molecules of OTf and that of OTf/2C is shown in Figure 7. For each half-molecule the signals due to both carbonyl carbons of the synergistic anion are split by $^1J(^{13}C\text{–}^{13}C)$ coupling (≈70–75 Hz) and $^2J(^{205}Tl\text{–}^{13}C)$ coupling (≈15–30 Hz) into two doublets of doublets ≈2 ppm apart, as illustrated in the figure. When the half-molecule was studied on a lower field instrument the separation in Hz between the mutliplets decreased (i.e., by a factor of $\approx 4/5$ in going from the AMX 500 to AM 400 instruments), while the peak separations within each multiplet remain the same, thus adding further credence to the assignment shown in Figure 7. Analogous ^{13}C NMR results were obtained for OTf/2N and the recombinant N-lobe of sTf (spectra not shown), and these are listed in Table 2 along with the data for OTf/2C. Since the magnitude of the two-bond $^{205}Tl\text{–}^{13}C$ spin–spin coupling is comparable for both carbons, we conclude that oxalate is coordinated to the metal ion in a 1,2-bidentate fashion in both OTf and sTf.

Field Dependence of sTf-Bound ^{205}Tl Signals. We have examined the transferrin-bound ^{205}Tl NMR signals for the Tl^{3+}/carbonate forms of sTf and OTf at two magnetic field strengths, 2.35 and 4.70 T (Figure 8). For each signal, an increase in field causes an appreciable increase in line width. This effect can be attributed to one of the relaxation mechanisms that are available to spin $I = {}^1/_2$ nuclei, namely, chemical shift anisotropy (CSA). This process, which involves fluctuating magnetic fields at the nucleus generated by anisotropies in the screening tensor σ and molecular tumbling, is markedly dependent on the strength of the external magnetic field. In general, the longitudinal (T_1) and transverse (T_2) relaxation times for a $I = {}^1/_2$ nucleus which relaxes by this pathway are given by the following relations (Farrar & Becker, 1971):

$$\frac{1}{T_1^{CSA}} = \frac{2}{15}\gamma^2 B_0{}^2 \Delta\sigma^2 \left\{ \frac{\tau_c}{1 + \gamma^2 B_0{}^2 \tau_c{}^2} \right\} \qquad (1)$$

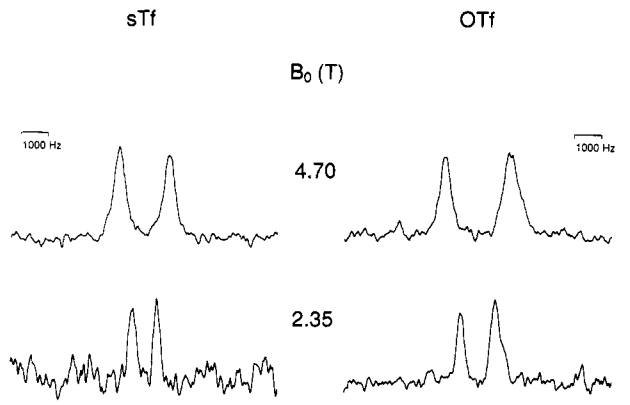

FIGURE 8: ^{205}Tl NMR spectra of $(Tl^{3+})_2$–OTf–$(CO_3^{2-})_2$ and $(Tl^{3+})_2$–sTf–$(CO_3^{2-})_2$ at two magnetic fields. (Lower traces) $B_0 = 2.35$ T ($\nu_0 = 57.7$ MHz); 1.04 mM sTf, 10 900 scans; 1.04 mM OTf, 41 200 scans. (Upper traces) $B_0 = 4.70$ T ($\nu_0 = 115.5$ MHz); 1.09 mM sTf, 58 400 scans; 1.20 mM OTf, 41 500 scans. Note that the width of each spectrum in frequency units (Hz) is identical.

$$\frac{1}{T_2^{CSA}} = \pi \Delta\nu_{1/2}{}^{CSA} = \frac{1}{15}\gamma^2 B_0{}^2 \Delta\sigma^2 \left\{ \frac{4}{3}\tau_c + \frac{\tau_c}{1 + \gamma^2 B_0{}^2 \tau_c{}^2} \right\} \qquad (2)$$

where γ is the magnetogyric ratio of the nucleus, B_0 is the magnetic field strength, $\Delta\sigma$ is the chemical shift anisotropy, and τ_c is the rotational correlation time.[3] Using the low-field (1.41 T) ^{205}Tl NMR data of Bertini *et al.* (1983), we plotted the line widths of the sTf-bound ^{205}Tl signals as a function of the square of the magnetic field (Figure 9). The data for both sites can be fit to a straight line ($r^2 = 0.98$). With the slopes of these curves and an average value for the empirical correlation time of bound metal ions in transferrins of 40 ns in hand (Aramini *et al.*, 1993; Aramini & Vogel, 1994; Schwab *et al.*, 1992), we used eq 2 to calculate a value for the chemical shift anisotropy for Tl^{3+} bound to the high-affinity iron-binding sites of sTf ($\Delta\sigma = 680$ ppm).[4] Since Tl^{3+} and the anion are bound in slow exchange to transferrins (*vide supra*; Bertini *et al.*, 1983), the $B_0{}^2$ dependence of the protein-bound ^{205}Tl line widths is due solely to CSA. These results also indicate that at $B_0 = 4.7$ T CSA is the dominant relaxation pathway for sTf-bound Tl^{3+}, although the nonzero y intercepts for both curves suggest that there is an important contribution to the ^{205}Tl line widths from another mechanism(s) (i.e., dipole–dipole relaxation).

DISCUSSION

The ^{205}Tl and ^{13}C NMR study of the transferrins presented here is an extension of the pioneering work in this area by Bertini *et al.* (1983, 1988) some time ago. From the ^{205}Tl NMR data for Tl^{3+} bound to these proteins we can draw several important conclusions regarding the nature and metal ion binding properties of the high-affinity binding sites in transferrins. First, the chemical shifts of the transferrin-bound ^{205}Tl NMR signals fall in a window ($\delta \approx 2100$–2050 ppm) that is intermediate between typical six-coordinate Tl^{3+} complexes where the metal ion is ligated by six oxygen atoms,

[3] In this expression, which is valid for axially symmetric molecules, $\Delta\sigma = \sigma_{||} - \sigma_{\perp}$, where $\sigma_{||}$ and $\sigma_{\perp}$ represent the screening tensors parallel and perpendicular to the symmetry axis.

[4] If τ_c is not known, then the field dependence of both T_1 and T_2 must be obtained in order to calculate $\Delta\sigma$ and τ_c using eqs 1 and 2. In addition, from eq 1, in the limit of slow molecular motion ($\omega_0\tau_c \gg 1$), $T_1{}^{CSA}$ is field independent; this certainly applies for ^{205}Tl bound to transferrins at both fields used in this study.

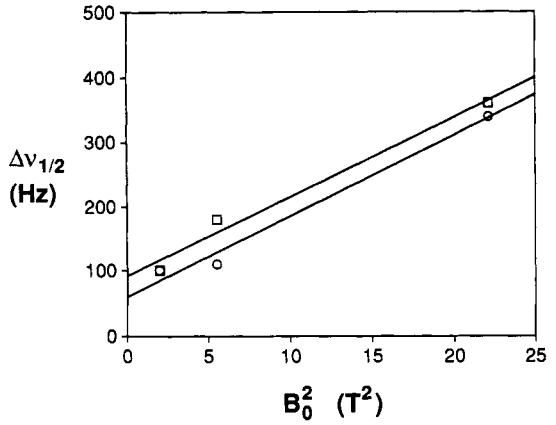

FIGURE 9: Plot of the sTf-bound ^{205}Tl signal line widths ($\Delta\nu_{1/2}$) against the square of the magnetic field strength (B_0^2). (□) N-site; (○) C-site.

such as $[Tl(oxalate)_3]^{3-}$, δ = 1951 ppm, and those where the metal ion is bound to two nitrogen- and four oxygen-containing ligands, like $[Tl(EDTA)]^-$, δ = 2281 ppm (Bertini *et al.*, 1983). On the basis of numerous spectroscopic and chemical modification studies, it was widely believed over a decade ago that two histidines acted as ligands for Fe^{3+} in both sites of a transferrin molecule [i.e., Pecoraro *et al.* (1981) and references therein]; hence, Bertini *et al.* proposed that their ^{205}Tl NMR data were consistent with the accepted dogma. However, it is now evident that the ^{205}Tl NMR resonance positions due to bound Tl^{3+} in ovo- and serotransferrin correlate well with the present picture, in which the metal ion is bound to one nitrogen (His) and five oxygen atoms (2 Tyr, 1 Asp, and the bidentate synergistic anion). Thus, in retrospect, accurate information regarding the ligand environment of the bound metal ion in the Fe^{3+}-binding sites of sTf was obtained by ^{205}Tl NMR spectroscopy 4 years before the first crystal structure of human lTf, demonstrating the potential of this technique as a probe for metalloproteins. Second, in the Tl^{3+}/carbonate forms of both sTf and OTf, the ^{205}Tl NMR signals due to the bound metal ion in the N- and C-sites are separated by δ = 17–21 ppm (Table 1), illustrating the extremely high sensitivity of the chemical shift of this nucleus to subtle differences in the Tl^{3+} environment. Moreover, the ^{205}Tl NMR data suggest that the local environment of the bound metal ion is virtually identical in the complementary lobes of both proteins. Third, the ^{205}Tl (and ^{13}C) NMR titration experiments reveal a discrepancy in the manner in which the transferrins studied here bind Tl^{3+}. In the case of sTf, Tl^{3+} is complexed with a higher affinity in the C-terminal lobe, while the sites in OTf exhibit no apparent difference in affinity for this metal ion. The results for sTf corroborate the large body of evidence indicating that the C-site is more adept than the N-site at accommodating larger cations, such as Gd^{3+}, Nd^{3+}, Sm^{3+}, and Th^{4+} (Zak & Aisen, 1988; Harris, 1986; Harris *et al.*, 1981; Luk, 1971). This disparity in the relative affinities of the sites in sTf for Tl^{3+} may account for the fact that, in mixed metal ion derivatives of this protein, Tl^{3+} remains in the C-site while Fe^{3+} occupies the N-site at physiological pH (Hinton *et al.*, 1988). Thus, Bertini *et al.* were misled in the assignment of the ^{13}C NMR signals of sTf by this approach, and with the benefit of recombinant sTf/2N we have obtained the correct solution (Table 1).

In addition to providing evidence in favor of a direct bond between the metal ion and anion in the metal ion binding sites of transferrins, the spin–spin couplings between the bound Tl^{3+} and anion detected by ^{13}C NMR can elucidate the mode of anion binding to the metal ion. While quite large values

Table 3: ^{13}C NMR Data for M^{3+}/Oxalate Adducts of OTf, sTf, and lTf

M^{3+}	protein	$\delta\ ^{13}C_1$ (ppm)	$\delta\ ^{13}C_2$ (ppm)	site	reference
Al^{3+}	OTf	168.47	165.89	N	Aramini and Vogel (1993a)
		168.42	165.33	C	
Al^{3+}	sTf	168.58	166.07	nd	Aramini, Saponja, and Vogel
		168.40	165.33	nd	(unpublished results)
Al^{3+}	lTf	168.55	166.0	nd	Aramini, Saponja, and Vogel
		168.24	166.0	nd	(unpublished results)
Ga^{3+}	OTf	168.4	166.2	N	Bertini *et al.* (1986)
		168.4	165.7	C	
Sc^{3+}	OTf	170.60	167.78	N	Aramini and Vogel (1994)
		170.52	167.00	C	
Tl^{3+}	OTf/2N	167.91	165.99		this study
Tl^{3+}	OTf/2C	167.80	165.35		this study
Tl^{3+}	sTf/2N	167.88	165.62		this study

of $^2J(^{205}Tl–^{13}C)$ are observed for the $Tl^{3+}/^{13}CO_3^{2-}$ forms of sTf, OTf, and their half-molecules, the magnitude of this coupling drops dramatically when oxalate serves as the synergistic anion. The comparable couplings between the metal ion and both carbonyl carbons of oxalate indicate that this anion is bound to Tl^{3+} in a 1,2-bidentate fashion. We attribute the surprising difference in the thallium–carbon couplings when the synergistic anion is oxalate vs carbonate to changes in the electronic nature and geometry of the metal-to-anion interaction (i.e., bidentate carbonate and the metal ion form a four-membered ring, whereas an extra carbonyl is inserted into the ring in the case of oxalate). The ^{13}C chemical shift data for the $Tl^{3+}/^{13}C_2O_4^{2-}$ adducts of OTf and sTf reported here are very similar to results obtained for the analogous complexes with other trivalent cations (Table 3). In each case, one observes two carbonyl signals, which are ≈2–3 ppm apart and at virtually identical positions in the spectrum. Thus, we propose that in transferrins oxalate also binds to other +3 metal ions in a 1,2-bidentate manner, in agreement with modeling studies (Baker *et al.*, 1990) and recent ESEEM (Dubach *et al.*, 1991) and X-ray data (Shongwe *et al.*, 1992) and not 1,1-bidentate or monodentate as previously proposed on the basis of ^{13}C NMR (Bertini *et al.*, 1986; Aramini & Vogel, 1993a). From the crystal structure of Cu^{2+}/oxalate bound to the C-site of lTf (Shongwe *et al.*, 1992) it is apparent that the chemical inequivalence of the two carbonyl carbons is due to differences in the nature of the protein residues that hydrogen-bond to each moiety. In particular, the oxygen of one carbonyl interacts with the guanidinium group of an arginine, while both oxygens of the other carbonyl are close enough to hydrogen-bond to a pair of amides at the N-terminus of a nearby α-helix; this may account for the differences in the magnitudes of the $^2J(^{205}Tl–^{13}C)$ couplings for the carbonyls of the same anion in each site.

Finally, the importance of the CSA mechanism in the relaxation of transferrin-bound Tl^{3+} has some major consequences. While our results are superior to the earlier ^{205}Tl NMR spectra of Bertini *et al.* on sTf at low field (1.41 T), by inspection of eq 2 it is obvious that a crucial consideration when contemplating the use of ^{205}Tl NMR to study macromolecules is the external magnetic field strength, B_0. From the slopes in Figure 9, a further doubling in B_0 to 9.4 T would result in signals with line widths greater than 10^3 Hz. Hence, to increase resolution one must sacrifice sensitivity and experiment time and choose a lower field instrument. The effectiveness of this mechanism precludes direct detection of spin–spin coupling between transferrin-bound Tl^{3+} and either carbonate or oxalate, and even for most small thallium

complexes such information must be obtained indirectly (i.e., by ^{1}H, ^{13}C, ^{31}P NMR; Hinton, 1992; Hinton *et al.*, 1988). The indirect detection of heteronuclear couplings has also been demonstrated for other $I = {}^{1}/_{2}$ metal nuclei, such as ^{113}Cd and ^{109}Ag, bound to small proteins by two-dimensional ^{1}H–X correlated NMR techniques (i.e., Frey *et al.*, 1985; Wörgötter *et al.*, 1988; Narula *et al.*, 1991). Another important factor is the size of the molecule, since line width varies linearly with τ_c. The magnitude of $\Delta\sigma$ also has a critical bearing on signal line width. The value of $\Delta\sigma$ for ^{205}Tl may be thousands of ppm (Hinton, 1992; Hinton *et al.*, 1988); hence, the result obtained for sTf is consistent with some degree of symmetry in the metal ion binding sites of this protein, in agreement with quadrupolar NMR studies of the transferrins (Aramini & Vogel, 1993a,b, 1994; Aramini *et al.*, 1993). While other heavy $I = {}^{1}/_{2}$ metal nuclei which possess favourable NMR traits, such as ^{195}Pt (Pregosin, 1986), ^{199}Hg (Wrakmeyer & Contreras, 1992), and ^{207}Pb (Wrackmeyer & Horchler, 1989), may be applied to the study of metalloproteins, one must be wary of the effects of CSA for such nuclei, which, like ^{205}Tl, exhibit vast chemical shift ranges. For example, we have observed ^{207}Pb line widths well in excess of 10^3 Hz at a field strength of 11.7 T for Pb^{2+} bound to the calcium-binding protein calmodulin (J. M. Aramini and H. J. Vogel, unpublished results). Indeed, the importance of CSA has been demonstrated for other $I = {}^{1}/_{2}$ metal nuclei bound to metalloproteins, such as ^{113}Cd (i.e., Kördel *et al.*, 1992) and even the low γ nucleus ^{57}Fe (Lee *et al.*, 1985).

ACKNOWLEDGMENT

We are indebted to Dr. A. B. Mason and Dr. R. C. Woodworth (University of Vermont, Burlington, VT) for providing us with a sample of recombinant sTf/2N. We thank Dr. C. Rodger (formerly with Bruker, Canada), Dr. M. W. Germann (Spectrospin AG, Fällanden, Switzerland), and Dr. D. Hughes (McMaster University, Hamilton, Ontario, Canada) for assisting us in acquiring ^{205}Tl NMR spectra. We also thank Ms. Jillian A. Saponja for her assistance in purifying the N- and C-terminal half-molecules of ovotransferrin.

REFERENCES

Anderson, B. F., Baker, H. M., Dodson, E. J., Norris, G. E., Rumball, S. V., Waters, J. M., & Baker, E. N. (1987) *Proc. Natl. Acad. Sci. U.S.A. 84*, 1769–1773.

Anderson, B. F., Baker, H. M., Norris, G. E., Rice, D. W., & Baker, E. N. (1989) *J. Mol. Biol. 209*, 711–734.

Anderson, B. F., Baker, H. M., Norris, G. E., Rumball, S. V., & Baker, E. N. (1990) *Nature 344*, 784–787.

Aramini, J. M., & Vogel, H. J. (1993a) *J. Am. Chem. Soc. 115*, 245–252.

Aramini, J. M., & Vogel, H. J. (1993b) *Bull. Magn. Reson. 15*, 84–88.

Aramini, J. M., & Vogel, H. J. (1994) *J. Am. Chem. Soc.* (in press).

Aramini, J. M., Germann, M. W., & Vogel, H. J. (1993) *J. Am. Chem. Soc. 115*, 9750–9753.

Bailey, S., Evans, R. W., Garratt, R. C., Gorinsky, B., Hasnain, S., Horsburgh, C., Jhoti, H., Lindley, P. F., Mydin, A., Sarra, R., & Watson, J. L. (1988) *Biochemistry 27*, 5804–5812.

Baker, E. N., & Lindley, P. F. (1992) *J. Inorg. Biochem. 47*, 147–160.

Baker, E. N., Anderson, B. F., Baker, H. M., Haridas, M., Norris, G. E., Rumball, S. V., & Smith, C. A. (1990) *Pure Appl. Chem. 62*, 1067–1070.

Battistuzzi, G., & Sola, M. (1992) *Biochim. Biophys. Acta 1118*, 313–317.

Bertini, I., Luchinat, C., & Messori, L. (1983) *J. Am. Chem. Soc. 105*, 1347–1350.

Bertini, I., Luchinat, C., Messori, L., Scozzafava, A., Pellacani, G., & Sola, M. (1986) *Inorg. Chem. 25*, 1782–1786.

Bertini, I., Messori, L., Pellacani, G. C., & Sola, M. (1988) *Inorg. Chem. 27*, 761–762.

Brock, J. H. (1985) in *Metalloproteins* (Harrison, P. M., Ed.) Part 2, pp 183–262, MacMillan Press, London.

Butler, A., & Eckert, H. (1989) *J. Am. Chem. Soc. 111*, 2802–2809.

Butler, A., Danzitz, M. J., & Eckert, H. (1987) *J. Am. Chem. Soc. 109*, 1864–1865.

de Jong, G., van Dijk, J. P., & van Eijk, H. G. (1990) *Clin. Chim. Acta 190*, 1–46.

Douglas, K. T., Bunni, M. A., & Baindur, S. R. (1990) *Int. J. Biochem. 22*, 429–438.

Dubach, J., Gaffney, B. J., More, K., Eaton, G. R., & Eaton, S. S. (1991) *Biophys. J. 59*, 1091–1100.

Evans, R. W., & Williams, J. (1978) *Biochem. J. 173*, 543–552.

Farrar, T. C., & Becker, E. D. (1971) *Pulse Fourier Transform NMR*, pp 46–65, Academic Press, New York.

Frey, M. H., Wagner, G., Vašák, M., Sørensen, O. W., Neuhaus, D., Wörgötter, E., Kägi, J. H. R., Ernst, R. R., & Wüthrich, K. (1985) *J. Am. Chem. Soc. 107*, 6847–6851.

Funk, W. D., MacGillivray, R. T. A., Mason, A. B., Brown, S. A., & Woodworth, R. C. (1990) *Biochemistry 29*, 1654–1660.

Grossmann, J. G., Neu, M., Pantos, E., Schwab, F. J., Evans, R. W., Townes-Andrews, E., Lindley, P. F., Appel, H., Thies, W.-G., & Hasnain, S. S. (1992) *J. Mol. Biol. 225*, 811–819.

Grossmann, J. G., Mason, A. B., Woodworth, R. C., Neu, M., Lindley, P. F., & Hasnain, S. S. (1993) *J. Mol. Biol. 231*, 554–558.

Harris, D. C. (1977) *Biochemistry 16*, 560–564.

Harris, D. C., & Aisen, P. (1989) in *Physical Bioinorganic Chemistry* (Loehr, T. M., Ed.) Vol. 5, pp 239–351, VCH Publishers, New York.

Harris, W. R. (1986) *Inorg. Chem. 25*, 2041–2045.

Harris, W. R., Carrano, C. J., Pecoraro, V. L., & Raymond, K. N. (1981) *J. Am. Chem. Soc. 103*, 2231–2237.

Heubers, H. A., & Finch, C. A. (1987) *Physiol. Rev. 67*, 520–582.

Hinton, J. F. (1992) *Bull. Magn. Reson. 13*, 90–108.

Hinton, J. F., Metz, K. R., & Briggs, R. W. (1988) *Prog. Nucl. Magn. Reson. Spectrosc. 20*, 423–513.

Kördel, J., Johansson, C., & Drakenberg, T. (1992) *J. Magn. Reson. 100*, 581–587.

Kubal, G., & Sadler, P. J. (1992) *J. Am. Chem. Soc. 114*, 1117–1118.

Kubal, G., Mason, A. B., Sadler, P. J., Tucker, A., & Woodworth, R. C. (1992) *Biochem. J. 285*, 711–714.

Kubal, G., Mason, A. B., Patel, S. U., Sadler, P. J., & Woodworth, R. C. (1993) *Biochemistry 32*, 3387–3395.

Lee, H. C., Gard, J. K., Brown, T. L., & Oldfield, E. (1985) *J. Am. Chem. Soc. 107*, 4087–4088.

Luk, C. K. (1971) *Biochemistry 10*, 2838–2843.

Mason, A. B., Funk, W. D., MacGillivray, R. T. A., & Woodworth, R. C. (1991) *Protein Expression Purif. 2*, 214–220.

Metz-Boutigue, M.-H., Jollès, J., Mazurier, J., Schoentgen, F., Legrand, D., Spik, G., Montreuil, J., & Jollès, P. (1984) *Eur. J. Biochem. 145*, 659–676.

Nakazato, K., Enami, I., Tanaka, Y., Uchiyama, Y., Tsugita, A., & Satake, K. (1992) *Biosci. Biotech. Biochem. 56*, 687–688.

Narula, S. S., Mehra, R. K., Winge, D. R., & Armitage, I. M. (1991) *J. Am. Chem. Soc. 113*, 9354–9358.

Oe, H., Doi, E., & Hirose, M. (1988) *J. Biochem. (Tokyo) 103*, 1066–1072.

Pecoraro, V. L., Harris, W. R., Carrano, C. J., & Raymond, K. N. (1981) *Biochemistry 20*, 7033–7039.

Pregosin, P. S. (1986) *Annu. Rep. NMR Spectrosc. 17*, 285–349.

Sarra, R., Garratt, R., Gorinsky, B., Jhoti, H., & Lindley, P. (1990) *Acta Crystallogr. B46*, 763–771.

Schlabach, M. R., & Bates, G. W. (1975) *J. Biol. Chem. 250*, 2182–2188.
Schwab, F. J., Appel, H., Neu, M., & Thies, W.-G. (1992) *Eur. Biophys. J. 21*, 147–154.
Shannon, R. D. (1976) *Acta Crystallogr. A32*, 751–767.
Shongwe, M. S., Smith, C. A., Ainscough, E. W., Baker, H. M., Brodie, A. M., & Baker, E. N. (1992) *Biochemistry 31*, 4451–4458.
Skoog, D. A., & West, D. M. (1982) *Fundamentals of Analytical Chemistry*, 4th ed., pp 749–752, Saunders College Publishing, New York.
Smith, C. A., Baker, H. M., & Baker, E. N. (1991) *J. Mol. Biol. 219*, 155–159.
Sola, M. (1990a) *Eur. J. Biochem. 194*, 349–353.
Sola, M. (1990b) *Inorg. Chem. 29*, 1113–1116.
Thornton, D. J., Holmes, D. F., Sheehan, J. K., & Carlstedt, I. (1989) *Anal. Biochem. 182*, 160–164.
Wörgötter, E., Wagner, G., Vašák, M., Kägi, J. H. R., & Wüthrich, K. (1988) *J. Am. Chem. Soc. 110*, 2388–2393.
Wrakmeyer, B., & Horchler, K. (1989) *Annu. Rep. NMR Spectrosc. 22*, 249–306.
Wrakmeyer, B., & Contreras, R. (1992) *Annu. Rep. NMR Spectrosc. 24*, 267–329.
Zak, O., & Aisen, P. (1988) *Biochemistry 27*, 1075–1080.
Zweier, J. L., Wooten, J. B., & Cohen, J. S. (1981) *Biochemistry 20*, 3505–3510.